CO Laser Absorption Coefficients for Gases of Biological Relevance: H_2O, CO_2, Ethanol, Acetaldehyde, and Ethylene

S. T. PERSIJN,* R. H. VELTMAN, J. OOMENS, F. J. M. HARREN, and D. H. PARKER

Department of Molecular and Laser Physics, Catholic University of Nijmegen, the Netherlands (S.T.P., J.O., F.J.M.H., D.H.P.); and ATO-DLO Wageningen, the Netherlands (R.H.V.)

The pressure-broadened spectra of water vapor, carbon dioxide, ethylene, ethanol, and acetaldehyde were recorded with the use of a liquid nitrogen-cooled CO laser-based photoacoustic spectrometer. The results obtained for CO_2 and H_2O gases were compared with those from the Hitran database. The absorption coefficients of ethylene, ethanol, and acetaldehyde on CO laser emission frequencies were determined as well. Finally, the measured spectra were used in a multicomponent analysis of trace gases released by pears (*Pyrus communis,* cultivar Conference).

Index Headings: **CO laser; Photoacoustic spectroscopy; Multicomponent analysis; Ethanol; Acetaldehyde; Ethylene.**

INTRODUCTION

Studies of trace amounts of volatile compounds released by biological samples may provide better insight into physiological processes occurring inside the tissue. Gas chromatography (GC), sometimes in combination with mass spectrometry, is widely used for this purpose. For some applications, however, GC has drawbacks such as limited sensitivity and a low time resolution. Preconcentration of gases emitted from the biological tissue, needed to overcome the limited sensitivity, lowers the time resolution and may also disturb the processes within the sample. Infrared laser-based photoacoustic (PA) detection, owing to its higher sensitivity, is an alternative for such applications, especially when dealing with small molecules.

The PA effect, discovered and described by Bell in 1880,[1] basically implies the conversion of light into acoustic energy. The intensity of the generated sound is proportional to the concentration of absorbing trace molecules. Kerr and Atwood performed the first trace gas analysis based on laser PA detection for trace gas analysis in 1968.[2] From that date, PA detection has proven a very sensitive method with applications in different fields. One example of trace gas analysis is the CO_2 laser-based PA detection of ethylene released by a single orchid flower; an impressive detection limit of 20 ppt (20 parts in 10^{12} volume) was achieved.[3]

The PA signal is proportional to the intensity of the incident laser beam and, therefore, high power sources, such as CO_2 lasers (λ = 9–11 μm, intracavity power up to 100 W) or CO lasers (λ = 5–8 μm, intracavity power up to 30 W), are required for sensitive trace gas detection.[4] Here we focus on the use of a CO laser; owing to its wide tuning range this laser is better suited for multicomponent analysis than the CO_2 laser.[5] Absorption of water vapor in the wavelength region of the CO laser causes interferences in particular when the analyte gas is present in relatively small amounts. In order to obtain reliable measurements, the concentration of water vapor in the incoming flow must be reduced; e.g., by leading the gas flow through a chemical scrubber or over a cold surface.

To conduct multicomponent analysis, one needs accurate knowledge of the absorption coefficients of gases under the investigation. Biological trace gas experiments are normally performed in a mixture of O_2 (between 0 and 21%) and N_2 as carrier gas; therefore, the measurement of the absorption coefficients was carried out in air and N_2 with, typically, a few hundred parts per million of the species diluted in the carrier gas. When using this approach, one encounters several complications. First, oxygen has its first vibrational level at 1554 cm^{-1}. Trace gases with a near-resonant vibrational level can transfer their vibrational energy to slowly relaxing oxygen, forming a buffer of vibrational energy and leading to a lower in-phase PA signal.[6] Second, pressure-shifting and pressure-broadening coefficients for water vapor absorption lines in air and nitrogen are different.[7–9]

This paper is concerned with measurement of absorption coefficients for H_2O, CO_2, ethylene (C_2H_4), ethanol (C_2H_5OH), and acetaldehyde (CH_3CHO) at CO laser frequencies. As such, the information obtained can be regarded as a contribution to the currently available bulk of data mainly for the following reasons:

- With the exception of water, only a very limited number of publications deal with measurement of absorption coefficients in the CO wavelength region.
- Most of the data were obtained with CO lasers operating at relatively high temperatures, causing only lines with a high rotational quantum number J to lase.[5] Operation at these lines is difficult, or even impossible, with a liquid nitrogen-cooled CO laser, where mainly low J-lines are accessible.[10–12]
- Published data usually relate data obtained at a total sample pressure below 1 bar,[10] whereas in practice measurements are commonly carried out at atmospheric pressures; pressure broadening can lead to significantly different results.

The absorption coefficients determined here were used in a multicomponent analysis of C_2H_4, CH_3CH_2OH, and CH_3CHO released by pears (*Pyrus communis,* cultivar Conference) under anaerobic conditions. Under aerobic conditions, the fruit produces its energy by respiration, i.e., the stepwise oxidation of sugars to form H_2O and

Received 22 April 1999; accepted 11 August 1999.
* Author to whom correspondence should be sent.

0003-7028/00/5401-0062$2.00/0

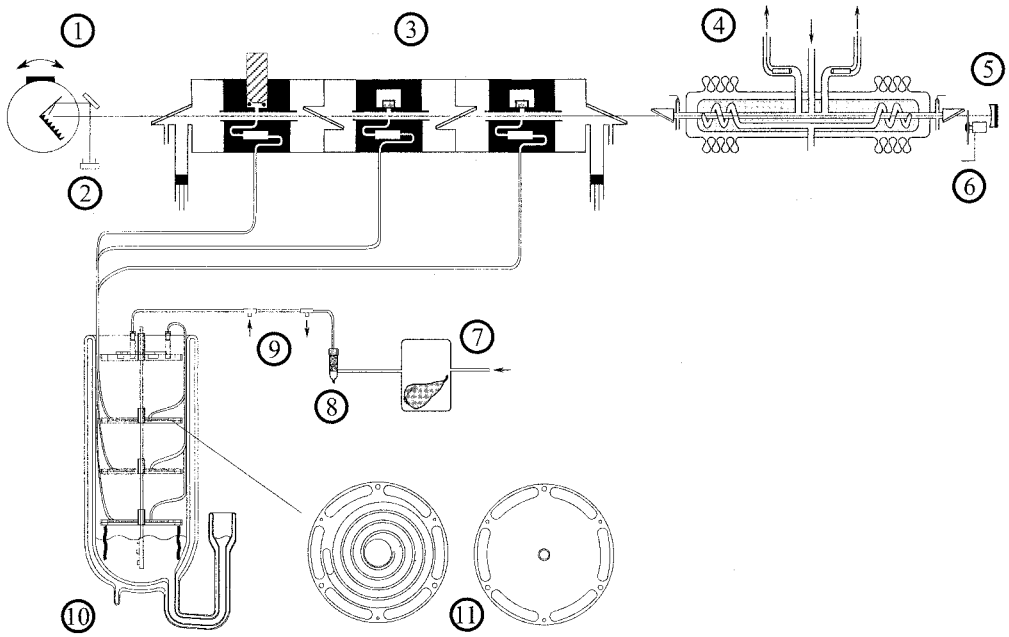

FIG. 1. CO laser-based photoacoustic spectrometer. **1**, Grating; **2**, pyroelectric detector **3**, triple photoacoustic cell; **4**, liquid nitrogen-cooled CO laser; **5**, 100% reflecting mirror; **6**, chopper; **7**, sample in cuvette; **8**, KOH scrubber; **9**, Nafion gas sample dryer; **10**, cold trap; **11**, detail showing cold trap plates.

CO_2 as end products. In order to prolong the storage period of harvested products, respiration is commonly reduced by exposure to reduced O_2 levels and temperature.[13] Currently, 40–50% of the Dutch pear harvest is stored under controlled atmosphere (CA) conditions. The production of ethylene, the only gaseous plant hormone that stimulates fruit ripening, also decreases at low O_2 levels.[14] At very low O_2 levels, however, an alternative metabolic process—alcoholic fermentation—takes place to provide the energy required by the fruit. Fermentation induces the production of ethanol and its precursor acetaldehyde, which can be monitored by means of the CO laser-based PA detector. Monitoring the emission of acetaldehyde, which is about 15 times more volatile than ethanol under ambient conditions,[15] yields information on the dynamics of alcoholic fermentation.

EXPERIMENTAL

Figure 1 shows the experimental setup (dimensions 3.5 $\times$ 0.5 $\times$ 0.6 m), which was thoroughly described elsewhere.[16] Here we restrict ourselves only to the most important features of the apparatus and new developments.

PA Cells. Three longitudinally resonant PA cells were mounted sequentially inside the laser cavity to enable as much as three samples to be analyzed simultaneously.[6,17] A very sensitive condenser microphone (1 V/Pa, Bruel & Kjaer 4179) is mounted in one of the cells; however, the large membrane of this microphone strongly influences the resonance frequency of this cell. Less sensitive electret microphones (22 mV/Pa, Knowless EK 3024) with a much smaller membrane are used in the other two cells. To match the resonance frequency for all three PA cells (diameter 15 mm for all resonators), the resonator length of the cell containing the sensitive microphone (total length 138 mm) was 8 mm shorter than that of the two other cells. With the cell filled with 1 atmosphere nitrogen, the resonance frequency is about 1130 Hz. A temperature control unit keeps the temperature of each PA cell slightly above that of the ambient, compensating for any additional differences in resonance frequency. Buffer volumes suppress the PA signal generated by absorption of laser radiation at Brewster windows. For optimal suppression, the length of the buffers is half of the resonator length. Two acoustical notch filters inserted into the gas inlet suppress acoustical noise from the surrounding laboratory. This arrangement results in a low background signal in the PA cell and a high sensitivity of approximately $2 \cdot 10^3$ Pa cm/W. The output of each microphone signal is fed into a lock-in amplifier with an integration time of typically 0.3 s. The phase of the PA signal is a measure for the vibrational-translational (V-T) relaxation time of the sample in a gas mixture; this relaxation time must be much shorter than the inverse of the modulation frequency (typically 0.9 ms) to avoid substantial phase lag between laser beam modulation and Pa signal.

CO Laser. The CO laser used here is similar to the design proposed by Urban's group at the University of Bonn.[18] Biologically important gases such as ethanol and ethylene absorb strongly around 7 μm, and therefore a CO laser operating at a low temperature is preferred for our experiments. This arrangement was achieved by using a 1.3 m long laser tube provided with a cooling jacket (a liquid nitrogen bath). However, the rotational temperature in a discharge is almost 100 K higher, (as derived from the *J*-dependency of the laser power), thereby decreasing the gain. The CO laser can be tuned over about 250 laser lines, yielding a single line emission between 5 and 7.9 μm by tilting the grating with a step motor (Oriel 18512). Multiple-line emission occurs only where different vibrational bands overlap, giving rise to less reliable measurements. The laser power is measured with

a pyroelectric detector at the zero-order reflection of the grating. The intracavity laser power was then calculated by multiplying the signal from the pyroelectric detector by a frequency-dependent correction factor. The latter was derived by comparing the known wavelength dependence of the commercially available outcoupling mirror at one end of the cavity and the zeroth-order reflection of the grating.[16]

Cold Trap. Water absorbing strongly over almost the entire wavelength region of the CO laser is always present in relatively large amounts. Many water scrubbers are commercially available; however, most of them to some extent also trap the analyte gas under study. The Nafion gas sample dryer (Perma Pure Inc., Model MD-050) operated in combination with a cold trap used in the multicomponent experiments removes water very efficiently. However, care should be exercised because ethanol, one of the detected trace gases, shows a tendency to stick to the Nafion membrane.

The newly designed three-level cold trap reduces the effect of water interference and increases the selectivity by trapping water and possibly other interfering volatiles. The cold trap consists of a Duran™ Dewar and four sets of two plates made of aluminum and stainless steel (see Fig. 1). Copper wires connected to the lowest level trap are immersed in liquid nitrogen at the bottom of the Dewar flask. Additional copper wires, interconnecting different levels of the trap, reduce the temperature of other levels. The incoming gas flow is first led to the upper level containing nine banana-shaped holes enclosing the tubes with a relatively large inner diameter. This level is kept at a temperature of about −10 °C to freeze out the major part of water vapor, thus preventing early obstruction of thin tubes at lower levels. Each of the outlet tubes at the upper level is connected to one of the three lower stages. The upper plate of each stage encloses thin tubes (ϕ 0.1 mm) in a long coil-shaped hole milled in the plate for optimal heat exchange (see detail in Fig. 1). The plates are temperature controlled by a sensor and a heater mounted on plates. For the moderate flows (up to 5 L/h) used in the experiments, the gas mixture in the tubes is at nearly the same temperature as the plates themselves. The temperatures of the lower, middle, and upper levels usually set to −170, −120, and −65 °C are stable within 0.5, 0.2, and 0.2 °C, respectively, as measured locally by the temperature sensors. The cold trap is automatically refilled approximately every 2 h. Filling from below by a funnel prevents large temperature fluctuations at upper traps by the incoming liquid nitrogen.

The lowest level trap can be used for detection of, e.g., ethylene and ethane, separating them from other gases such as water, ethanol, and acetaldehyde. Many other gases have vapor pressures below the ppb level at this temperature, thus allowing a precise concentration measurement. The −120 °C level trap is used for measurements with acetaldehyde and CO_2, while the −65 °C trap must be utilized in series of ethanol measurements. Therefore, ethanol concentration measurements generally possess a rather high uncertainty due to a large interference with other gases at such relatively high temperature (especially water, with a partial vapor pressure of around 5 ppm at −65 °C).

MULTICOMPONENT ANALYSIS

The PA trace gas detector is fully computer controlled and capable of measuring several gases quasi-simultaneously, i.e., within a time span of several minutes. The PA signal on a single laser line is the sum of the contributions of each constituent gas (that absorbs at this laser line) and a background signal. This latter is mainly due to heating of windows and absorption of laser radiation by the resonator wall. To calculate the concentrations of n absorbing trace gases, it is necessary to record the amplitude of the PA signal (in case of fast relaxing gas mixtures, phase information can be omitted) on N laser lines, with $N \geq n + 1$. The PA signal S_i on line i (in V) is given by

$$S_i = F \cdot P_i \cdot \left[b_i + \sum_{j=1}^{n} C_j \alpha_{ij} \right] \qquad (1)$$

where F is the cell constant (in cm V/W); C_j is the partial pressure of gas j (in atm); α_{ij} is the absorption coefficient of gas j on line i (in $atm^{-1}\,cm^{-1}$); b_i is the background signal on line i (in cm^{-1}); and P_i is the intracavity laser power (in W). In the ideal case, there is a unique solution to this set of linear equations. In practice, however, there do exist sources of errors such as acoustical noise (important only for very low PA signals), absorption of remaining trace gases not taken into account in the calculation, errors in the absorption coefficients, and possibly strongly varying concentrations during a measurement cycle. If not all constituents in the gas mixture are known, a complete spectrum must be recorded, revealing all absorbing constituents.

In fact, the PA signal is a vector quantity containing phase and amplitude information. However, since nearly all experiments were performed in rapidly relaxing gas mixtures (low O_2/high H_2O vapor), the phase of the signal was fairly constant (and thus contained little information). Therefore, the applied algorithm to calculate the concentration of each compound[16,19] based on Eq. 1 is adequate for our purposes. In general, an overdetermined ($N > n + 1$) set of equations is preferred to reduce the error in calculated concentrations. However, for rapidly varying concentrations, the measuring time per cycle should be as short as possible. In this case, it is better to reduce the number of laser lines since it takes up to 1 min to sample the PA signal on each laser line and move the grating with the step motor to the next laser line.

DETERMINATION OF ABSORPTION COEFFICIENTS

The PA spectra of H_2O, CO_2, ethanol, acetaldehyde, and ethylene gases and the background PA signal were recorded by scanning the laser over all emission lines at a PA cell temperature of 298–300 K and a pressure slightly above the atmospheric one. Each spectrum was recorded several times (typically five), and average values for absorption coefficients (with their standard deviations) were determined at each laser line.

The absorption coefficients of H_2O were determined first; the strong ν_2 bending mode of H_2O is centered at 1595 cm^{-1}. Water contributes significantly to the PA signal due to this strong absorption, even if the coldest level

TABLE I. Absorption coefficients (in atm^{-1} cm^{-1}) of water, CO_2, ethylene, acetaldehyde, and ethanol diluted in nitrogen. The standard deviation of the data (in parentheses) is in the units of the last digit. A dash (—) indicates that no absorption coefficient could be determined due to, e.g., weak absorption, high water interference, or low laser power. An asterisk (*) marks six laser lines that are used in the multicomponent analysis. Furthermore, absorption coefficients as calculated from the Hitran database are given for water and CO_2.

Laser line	Frequency (cm^{-1})	H_2O (atm^{-1} cm^{-1})	H_2O Hitran	CO_2 (atm^{-1} cm^{-1})	CO_2 Hitran	Ethylene (atm^{-1} cm^{-1})	Acetaldehyde (atm^{-1} cm^{-1})	Ethanol (atm^{-1} cm^{-1})
v31j10	1328.80481	1.44 (3)·10⁻²	1.25·10⁻³	—	—	—	3.7 (7)	1.2 (3)·10⁻¹
v31j9	1331.87549	1.11 (6)·10⁻²	1.33·10⁻³	—	—	1.6 (1)·10⁻³	5 (2)	1.1 (4)
v31j8	1334.91235	1.3 (1)·10⁻²	2.18·10⁻³	—	—	—	5 (2)	1.2 (2)
v31j7	1337.91528	1.82 (2)·10⁻¹	1.76·10⁻¹	—	—	—	1.0 (2)·10¹	1.4 (6)
v31j6	1340.88428	8.7 (5)·10⁻²	4.52·10⁻²	—	—	—	7 (2)·10⁻¹	1.4 (2)
v30j12	1346.3717	1.4 (1)·10⁻²	1.28·10⁻³	—	—	—	—	2 (1)
v30j11	1349.54407	5.1 (7)·10⁻²	4.56·10⁻²	4.8 (9)·10⁻⁵	2.48·10⁻⁵	—	6 (3)	—
v30j10	1352.68286	7.6 (3)·10⁻³	2.13·10⁻³	2.1 (1)·10⁻⁴	2.05·10⁻⁴	2.7 (2)·10⁻³	6 (1)	1.5 (2)
v30j9	1355.78821	1.23 (9)·10⁻²	4.87·10⁻³	5.9 (1)·10⁻⁵	4.35·10⁻⁵	3.6 (2)·10⁻³	3.2 (6)	1.8 (4)
v30j8	1358.85974	1.6 (2)·10⁻²	6.22·10⁻³	4.4 (8)·10⁻⁵	2.38·10⁻⁵	2.03 (6)·10⁻³	4.3 (6)	2.5 (8)
v30j7	1361.89746	4.4 (2)·10⁻²	2.71·10⁻²	—	—	3.2 (2)·10⁻³	7 (2)	2.7 (9)
v30j6	1364.90112	2.7 (2)·10⁻²	6.94·10⁻³	—	—	—	—	3.2 (5)
v29j13	1366.98938	4.0 (6)·10⁻²	4.29·10⁻³	—	—	—	1.5 (3)	—
v29j11	1373.4364	1.37 (1)·10⁻¹	1.47·10⁻¹	—	—	—	6 (1)	4 (1)
v29j10	1376.60999	1.55 (9)·10⁻²	8.37·10⁻³	5.3 (4)·10⁻⁵	3.47·10⁻⁵	1.28 (4)·10⁻²	4.6 (7)	6 (3)
v29j9	1379.74988	4.43 (7)·10⁻²	4.88·10⁻²	8.9 (9)·10⁻⁵	4.21·10⁻⁵	3.5 (6)·10⁻²	4.7 (6)	6 (1)
v29j8	1382.8562	1.17 (8)·10⁻²	3.71·10⁻³	1.1 (5)·10⁻⁴	8.35·10⁻⁵	1.542 (8)·10⁻¹	4.2 (5)	6 (1)
v29j7	1385.92859	3.6 (2)·10⁻²	2.52·10⁻²	1.55 (6)·10⁻⁴	1.37·10⁻⁴	1.1 (4)·10⁻¹	3.9 (7)	5 (1)
v29j6	1388.96704	2.7 (1)·10⁻²	1.56·10⁻²	—	—	—	5 (1)	4.2 (6)
v28j12	1394.14197	2.6 (1)·10⁻¹	3.02·10⁻¹	—	—	—	—	10 (6)
v28j11	1397.38342	4.6 (1)·10⁻²	4.03·10⁻²	7.5 (2)·10⁻⁵	6.59·10⁻⁵	2.7 (3)·10⁻¹	2.8 (4)	5 (2)
v28j10	1400.59167	3.00 (6)·10⁻²	2.38·10⁻²	2.8 (2)·10⁻⁵	1.02·10⁻⁵	2.24 (1)·10⁻¹	3.9 (4)	—
v28j9	1403.76636	2.71 (9)·10⁻²	1.76·10⁻²	2.4 (1)·10⁻⁵	5.13·10⁻⁶	4.5 (2)·10⁻¹	4.7 (7)	7 (2)
v28j8*	1406.90735	1.4 (6)·10⁻²	7.76·10⁻³	2.61 (6)·10⁻⁵	9.66·10⁻⁶	5.8 (3)·10⁻¹	4.7 (4)	7 (2)
v28j7	1410.01453	1.12 (2)·10⁻¹	1.58·10⁻¹	3.6 (3)·10⁻⁵	2.73·10⁻⁶	9.2 (2)·10⁻¹	4.7 (5)	5 (1)
v28j6	1413.08777	1.2 (6)·10⁻²	5.66·10⁻³	—	—	—	6 (1)	3.9 (8)
v27j13	1414.80469	2.12 (5)·10⁻²	1.82·10⁻²	—	—	—	9 (2)	4 (2)
v28j5	1416.12695	4.8 (2)·10⁻¹	5.24·10⁻¹	—	—	—	7 (2)	—
v27j12	1418.11401	7.4 (2)·10⁻²	7.66·10⁻²	—	—	—	4.8 (8)	3 (2)
v27j11	1421.39026	3.51 (6)·10⁻²	2.85·10⁻²	1.2 (1)·10⁻⁵	1.43·10⁻⁷	7.9 (4)·10⁻¹	4.5 (5)	3.0 (8)
v27j10	1424.63318	5.2 (2)·10⁻²	4.71·10⁻²	1.1 (2)·10⁻⁵	—	1.33 (1)	3.8 (4)	2.5 (8)
v27j9	1427.84253	2.08 (5)·10⁻²	1.58·10⁻²	8 (1)·10⁻⁶	—	1.04 (6)	3.0 (3)	2.0 (6)
v27j8	1431.01831	2.72 (6)·10⁻²	2.54·10⁻²	9 (1)·10⁻⁶	—	2.85 (4)·10⁻¹	2.5 (2)	1.6 (4)
v27j7	1434.16028	2.71 (8)·10⁻²	2.25·10⁻²	8 (2)·10⁻⁶	—	2.3 (1)·10⁻¹	2.1 (2)	1.6 (4)
v27j6	1437.26843	4.2 (2)·10⁻¹	4.37·10⁻¹	4.7 (8)·10⁻⁵	—	3.9 (2)·10⁻¹	4.0 (6)	1.5 (6)
v27j5	1440.34241	2.7 (1)·10⁻²	1.07·10⁻²	—	—	—	6 (2)	1.5 (1)
v26j12*	1442.15064	1.32 (4)·10⁻²	6.79·10⁻³	1.5 (4)·10⁻⁵	—	3.5 (3)·10⁻¹	3.3 (4)	1.96 (8)
v26j11*	1445.46155	1.73 (3)·10⁻²	1.15·10⁻²	1.2 (2)·10⁻⁵	—	1.92 (8)	3.0 (3)	1.8 (4)
v26j10	1448.73914	5 (2)·10⁻²	5.19·10⁻²	1.8 (2)·10⁻⁵	—	4.4 (1)·10⁻¹	2.8 (3)	1.8 (4)
v26j9	1451.98328	3.9 (2)·10⁻¹	4.84·10⁻¹	5.1 (6)·10⁻⁵	—	7.5 (4)·10⁻¹	2.1 (2)	1.7 (5)
v26j8	1455.19385	6.2 (3)·10⁻¹	6.85·10⁻¹	5.8 (6)·10⁻⁵	—	3.3 (1)·10⁻¹	1.9 (1)	1.6 (7)
v26j7	1458.37061	2.3 (4)	2.27	1.6 (1)·10⁻⁴	—	1.09 (2)	1.8 (3)	1.3 (3)
v26j6	1461.51355	3.3 (1)·10⁻²	2.34·10⁻²	—	—	2 (1)·10⁻¹	2.1 (3)	1.3 (4)
v25j13	1462.87659	3.39 (9)·10⁻²	2.81·10⁻²	—	—	—	—	1.2 (4)
v25j12	1466.25549	4.74 (7)·10⁻²	4.56·10⁻²	1.1 (4)·10⁻⁵	—	7.2 (4)·10⁻¹	1.5 (2)	1.44 (8)
v25j11	1469.6012	2.79 (9)·10⁻²	2.56·10⁻²	1.07 (3)·10⁻⁵	—	6.9 (2)·10⁻¹	1.3 (1)	1.1 (2)
v25j10	1472.91357	2.4 (8)·10⁻¹	2.71·10⁻¹	1.5 (3)·10⁻⁵	—	4.84 (3)·10⁻¹	1.5 (1)	1.0 (5)
v25j9	1476.19251	2.2 (4)	2.37	9 (2)·10⁻⁵	—	1.17 (2)	1.7 (5)	—
v25j8	1479.43787	1.82 (6)·10⁻²	1.27·10⁻²	3.5 (5)·10⁻⁶	—	5.71 (4)·10⁻¹	8 (9)·10⁻¹	9 (5)·10⁻¹
v25j7	1482.64941	2.04 (4)·10⁻²	1.59·10⁻²	5.2 (3)·10⁻⁶	—	5.7 (5)·10⁻¹	8 (1)·10⁻¹	1.0 (4)
v25j6	1485.82715	4.9 (1)·10⁻²	4.78·10⁻²	6.5 (8)·10⁻⁶	—	4.44 (8)·10⁻¹	1.0 (2)·10⁻¹	8 (3)·10⁻¹
v24j12	1490.43225	2.54 (4)·10⁻¹	2.93·10⁻¹	—	—	3.0 (2)·10⁻¹	7.1 (8)·10⁻¹	—
v24j11*	1493.81274	3.09 (9)·10⁻²	2.96·10⁻²	—	—	2.792 (4)·10⁻¹	7 (1)·10⁻¹	6 (4)·10⁻¹
v24j10	1497.15991	1.12 (4)·10⁻¹	1.41·10⁻¹	8 (1)·10⁻⁶	—	1.41 (4)·10⁻¹	7.2 (6)·10⁻¹	5 (1)·10⁻¹
v24j9	1500.47376	8.8 (3)·10⁻²	9.13·10⁻²	8 (1)·10⁻⁶	—	6.9 (1)·10⁻²	6.6 (6)·10⁻¹	5 (1)·10⁻¹
v24j8	1503.75391	6.9 (2)·10⁻²	7.25·10⁻²	7 (2)·10⁻⁶	—	5 (4)·10⁻²	7.1 (8)·10⁻¹	5 (2)·10⁻¹
v23j13	1511.23547	6.6 (2)·10⁻²	6.99·10⁻²	—	—	—	6 (1)·10⁻¹	4 (2)·10⁻¹
v23j12	1514.68396	1.55 (3)·10⁻¹	1.75·10⁻¹	—	—	1.07 (3)·10⁻²	4.8 (4)·10⁻¹	3.4 (8)·10⁻¹
v23j11	1518.09937	1.63 (4)·10⁻¹	2.07·10⁻¹	—	—	—	6 (2)·10⁻¹	—
v23j10	1521.48132	2.9 (8)	2.84	—	—	1 (1)·10⁻³	1.0 (6)	—
v23j9	1524.82996	6.8 (2)·10⁻¹	2·10⁻¹	—	—	2.7 (7)·10⁻³	5 (1)·10⁻¹	2 (1)·10⁻¹
v23j8	1528.14502	1.43 (5)·10⁻¹	1.39·10⁻¹	—	—	1.8 (2)·10⁻³	4.5 (4)·10⁻¹	1.4 (3)·10⁻¹
v22j13	1535.52991	2.3 (1)·10⁻¹	3.28·10⁻¹	—	—	—	7 (2)·10⁻¹	—
v22j11	1542.4635	8.6 (1)·10⁻¹	1.05	—	—	—	4 (2)·10⁻¹	—
v22j10	1545.88037	2.04 (7)·10⁻¹	2.04·10⁻¹	—	—	1.5 (4)·10⁻⁴	3.9 (4)·10⁻¹	—
v22j9	1549.26379	1.42 (3)·10⁻¹	—	—	—	—	4.8 (4)·10⁻¹	—
v22j8	1552.61377	6.3 (2)·10⁻²	6.19·10⁻²	—	—	3.7 (1)·10⁻⁴	5 (6)·10⁻¹	7 (2)·10⁻²
v22j7	1555.92993	1.35 (4)·10⁻¹	1.65·10⁻¹	—	—	5 (1)·10⁻⁴	4.7 (5)·10⁻¹	—
v21j14	1556.35278	1.3 (4)·10⁻¹	1.51·10⁻¹	—	—	6 (1)·10⁻⁴	3.4 (3)·10⁻¹	9 (7)·10⁻²

TABLE I. Continued

Laser line	Frequency (cm^{-1})	H_2O ($atm^{-1}\ cm^{-1}$)	H_2O Hitran	CO_2 ($atm^{-1}\ cm^{-1}$)	CO_2 Hitran	Ethylene ($atm^{-1}\ cm^{-1}$)	Acetaldehyde ($atm^{-1}\ cm^{-1}$)	Ethanol ($atm^{-1}\ cm^{-1}$)
v22j6	1559.21228	6.4 (1)·10⁻¹	7.89·10⁻¹	—	—	—	5.7 (9)·10⁻¹	—
v21j12	1563.42212	5.13 (9)·10⁻²	5.63·10⁻²	—	—	3.8 (4)·10⁻⁴	3.7 (5)·10⁻¹	5 (1)·10⁻²
v21j11	1566.90723	3.52 (7)·10⁻²	3.4·10⁻²	—	—	2.2 (2)·10⁻⁴	3.5 (4)·10⁻¹	7 (3)·10⁻²
v21j10	1570.35913	2.5 (4)·10⁻¹	2.65·10⁻¹	—	—	—	3.2 (3)·10⁻¹	—
v21j9	1573.77747	5 (8)·10⁻²	4.95·10⁻²	—	—	1.4 (6)·10⁻³	2.9 (3)·10⁻¹	6 (2)·10⁻²
v21j8	1577.16223	2.2 (4)·10⁻¹	2.62·10⁻¹	—	—	2.5 (3)·10⁻⁴	2.8 (3)·10⁻¹	—
v21j7	1580.51331	1.57 (4)·10⁻²	1.58·10⁻²	—	—	7.9 (6)·10⁻⁴	2.7 (4)·10⁻¹	5 (2)·10⁻²
v21j6	1583.83057	9.7 (3)·10⁻³	7.73·10⁻³	—	—	5.3 (2)·10⁻⁴	2.7 (3)·10⁻¹	6 (1)·10⁻²
v21j5	1587.11377	9.1 (2)·10⁻³	6.13·10⁻³	—	—	5.7 (3)·10⁻⁴	3.2 (4)·10⁻¹	5 (2)·10⁻²
v20j12	1587.91248	1.04 (2)·10⁻²	4.77·10⁻³	—	—	5.1 (7)·10⁻⁴	2.7 (3)·10⁻¹	7 (4)·10⁻²
v20j11	1591.4325	2.75 (5)·10⁻²	2.19·10⁻²	—	—	4.5 (3)·10⁻⁴	2.8 (3)·10⁻¹	7 (3)·10⁻²
v20j10	1594.91931	3.58 (9)·10⁻²	3.16·10⁻²	—	—	3.41 (4)·10⁻⁴	2.8 (3)·10⁻¹	6 (4)·10⁻²
v20j9	1598.37256	9.6 (3)·10⁻³	4.57·10⁻³	—	—	1.77 (9)·10⁻⁴	2.4 (3)·10⁻¹	5 (2)·10⁻²
v20j8	1601.79224	1.61 (3)·10⁻²	1.29·10⁻²	—	—	2.5 (1)·10⁻⁴	2.5 (3)·10⁻¹	5 (2)·10⁻²
v20j7	1605.17822	1.07 (4)·10⁻²	6.7·10⁻³	—	—	5.1 (2)·10⁻⁴	2.4 (3)·10⁻¹	6 (3)·10⁻²
v20j6	1608.5304	3.07 (5)·10⁻²	1.8·10⁻²	—	—	3.7 (1)·10⁻⁴	2.9 (3)·10⁻¹	6 (3)·10⁻²
v19j13	1608.89746	3.21 (9)·10⁻²	3.49·10⁻²	—	—	3.71 (4)·10⁻⁴	2.5 (2)·10⁻¹	5 (2)·10⁻²
v19j12	1612.4856	2.2 (4)·10⁻²	1.69·10⁻²	—	—	3.4 (2)·10⁻⁴	2.6 (3)·10⁻¹	6 (2)·10⁻²
v19j11*	1616.04053	3.99 (4)·10⁻¹	4.33·10⁻¹	—	—	2 (1)·10⁻⁴	3.0 (7)·10⁻¹	—
v19j10	1619.56226	3.72 (6)·10⁻²	3.75·10⁻²	—	—	6.3 (1)·10⁻⁴	2.5 (2)·10⁻¹	5 (2)·10⁻²
v19j9	1623.05041	2.43 (4)·10⁻¹	2.86·10⁻¹	—	—	2.1 (1)·10⁻⁴	2.0 (4)·10⁻¹	—
v19j8	1626.50513	3.44 (8)·10⁻²	3.43·10⁻²	—	—	3.2 (3)·10⁻⁴	2.2 (2)·10⁻¹	4 (2)·10⁻²
v19j7	1629.92603	2.35 (8)·10⁻²	1.99·10⁻²	—	—	3.2 (2)·10⁻⁴	2.3 (2)·10⁻¹	6 (3)·10⁻²
v18j14	1629.86328	2.4 (6)·10⁻²	2.04·10⁻²	—	—	3.3 (3)·10⁻⁴	2.4 (1)·10⁻¹	6 (2)·10⁻²
v18j13	1633.51941	6.1 (2)·10⁻²	6.06·10⁻²	—	—	1.8 (6)·10⁻⁴	2.43 (8)·10⁻¹	—
v18j12	1637.14246	2.39 (4)·10⁻¹	2.46·10⁻¹	—	—	4 (2)·10⁻⁵	2.4 (5)·10⁻¹	5 (2)·10⁻²
v18j11	1640.7323	4.13 (8)·10⁻²	3.75·10⁻²	—	—	3.8 (3)·10⁻⁴	2.22 (1)·10⁻¹	5 (2)·10⁻²
v18j10	1644.28894	5.7 (1)·10⁻²	6.17·10⁻²	—	—	3.4 (3)·10⁻⁴	1.92 (8)·10⁻¹	5 (3)·10⁻²
v18j9	1647.81213	3.34 (4)·10⁻¹	3.68·10⁻¹	—	—	—	1.3 (7)·10⁻¹	—
v18j8	1651.30176	2.05 (4)·10⁻¹	2.33·10⁻¹	—	—	3 (1)·10⁻⁴	1.6 (4)·10⁻¹	—
v18j7	1654.75757	1.18 (6)	1.08	—	—	—	4 (1)·10⁻¹	5 (2)·10⁻²
v17j13	1658.22559	3.48 (5)·10⁻²	2.88·10⁻²	—	—	4.9 (2)·10⁻⁴	2.36 (9)·10⁻¹	6 (4)·10⁻²
v17j12	1661.88367	8.8 (2)·10⁻²	9.3·10⁻²	—	—	2.9 (5)·10⁻⁴	2.2 (1)·10⁻¹	7 (4)·10⁻²
v17j11	1665.50854	2.53 (6)·10⁻²	2.5·10⁻²	—	—	4.0 (3)·10⁻⁴	2.28 (10)·10⁻¹	5 (2)·10⁻²
v17j10	1669.1001	1.9 (4)	1.88	—	—	—	3.9 (10)·10⁻¹	5 (2)·10⁻²
v17j9	1672.65833	8.6 (3)·10⁻²	7.69·10⁻²	—	—	5.1 (9)·10⁻⁴	3.08 (1)·10⁻¹	5 (4)·10⁻²
v17j8	1676.18286	1.8 (5)·10⁻¹	1.57·10⁻¹	—	—	8 (2)·10⁻⁴	4 (2)·10⁻¹	—
v17j7	1679.67371	2.5 (2)·10⁻¹	3.21·10⁻¹	—	—	1.24 (5)·10⁻³	5.2 (4)·10⁻¹	7 (2)·10⁻²
v16j12	1686.7096	8.8 (2)·10⁻²	9.19·10⁻²	—	—	7.4 (9)·10⁻⁴	7.0 (6)·10⁻¹	5 (2)·10⁻²
v16j11	1690.36951	2.18 (9(·10⁻¹	2.36·10⁻¹	—	—	1.1 (3)·10⁻³	2.0 (4)·10⁻¹	—
v16j10	1693.99609	7.8 (2)·10⁻²	8.33·10⁻²	—	—	2.4 (1)·10⁻³	1.08 (4)	5 (3)·10⁻²
v16j9	1697.58923	9.01 (4)·10⁻¹	9.64·10⁻¹	—	—	—	1.2 (2)	5 (2)·10⁻²
v16j8	1701.14868	1.9 (6)	1.88	—	—	—	1.5 (5)	5 (2)·10⁻²
v15j14	1704.13123	5.17 (9)·10⁻¹	3.75·10⁻¹	—	—	3.32 (9)·10⁻³	2.9 (2)	8 (7)·10⁻²
v16j7	1704.67456	5.9 (2)·10⁻¹	6.99·10⁻¹	—	—	2.7 (1)·10⁻³	2.6 (2)	6 (3)·10⁻²
v15j13	1707.89221	3.5 (9)·10⁻²	4.08·10⁻²	—	—	1.83 (6)·10⁻³	2.8 (2)	5 (2)·10⁻²
v15j12	1711.62036	2.5 (4)·10⁻²	2.41·10⁻²	—	—	5.8 (2)·10⁻³	3.6 (3)	6 (3)·10⁻²
v15j11	1715.31519	1.28 (3)	1.29	—	—	4 (1)·10⁻³	5.6 (3)	—
v15j10	1718.97681	7.1 (1)·10⁻¹	6.86·10⁻¹	—	—	1.9 (6)·10⁻³	8.4 (3)	—
v15j9	1722.60498	3.63 (9)·10⁻²	3.15·10⁻²	—	—	1.14 (7)·10⁻²	1.9 (6)·10¹	6 (2)·10⁻²
v15j8	1726.19946	1.79 (4)·10⁻²	1.46·10⁻²	—	—	1.46 (5)·10⁻²	1.3 (1)·10¹	8 (3)·10⁻²
v14j14	1729.0564	3.45 (8)·10⁻¹	3.67·10⁻²	—	—	4.6 (5)·10⁻³	1.7 (1)·10¹	8 (7)·10⁻²
v15j7	1729.76013	5.7 (2)·10⁻¹	7.55·10⁻¹	—	—	3.3 (2)·10⁻³	1.63 (8)·10¹	6 (2)·10⁻²
v14j13	1732.85254	9.1 (1)·10⁻¹	2.61·10⁻¹	—	—	1.11 (5)·10⁻²	1.51 (5)·10¹	—
v15j6	1733.28711	1.17 (3)	4.54	—	—	1.16 (7)·10⁻²	1.41 (5)·10¹	—
v14j12	1736.6156	4.42 (10)·10⁻²	4.89·10⁻²	—	—	9.6 (1)·10⁻³	1.5 (1)·10¹	4 (2)·10⁻²
v14j11	1740.34546	2.81 (5)·10⁻¹	2.75·10⁻¹	—	—	4.7 (2)·10⁻³	1.56 (8)·10¹	5.1 (1)·10⁻²
v14j10	1744.04211	9.1 (2)·10⁻²	7.73·10⁻²	—	—	5.3 (3)·10⁻³	1.8 (1)·10¹	—
v14j9	1747.7052	5 (1)·10⁻¹	6.23·10⁻¹	—	—	4.0 (3)·10⁻³	1.59 (7)·10¹	—
v14j8	1751.33472	3.28 (4)	3.08	—	—	—	1.12 (8)·10¹	—
v13j14	1754.93042	1.61 (3)·10⁻²	1.55·10⁻²	—	—	1.1 (1)·10⁻²	2.0 (1)·10¹	8 (2)·10⁻²
v14j7	1754.93042	1.78 (5)·10⁻²	1.55·10⁻²	—	—	9.2 (2)·10⁻³	1.63 (8)·10¹	—
v13j13	1757.89685	5.8 (1)·10⁻²	3.43·10⁻²	—	—	6.3 (1)·10⁻³	2.2 (1)·10¹	7 (3)·10⁻²
v13j12	1761.69495	1.7 (2)	2.05	—	—	5 (2)·10⁻³	2.29 (9)·10¹	—
v13j11*	1765.45984	2.19 (6)·10⁻²	2.13·10⁻²	—	—	7.9 (2)·10⁻³	2.1 (1)·10¹	8 (1)·10⁻²
v13j10	1769.19153	4.3 (1)·10⁻²	3.74·10⁻²	—	—	3.53 (3)·10⁻³	1.51 (9)·10¹	—
v13j9	1772.88965	2.57 (9)	2.54	—	—	4 (3)·10⁻³	1.04 (7)·10¹	—
v13j8	1776.55408	2.3 (5)·10⁻²	2.31·10⁻²	—	—	1.727 (3)·10⁻²	7.3 (4)	6 (1)·10⁻²
v12j14	1779.15833	9 (2)·10⁻²	2.59·10⁻¹	—	—	6.18 (2)·10⁻³	7.8 (5)	9 (4)·10⁻²
v13j7	1780.18481	6.6 (2)·10⁻²	7.52·10⁻²	—	—	5.59 (8)·10⁻³	6.1 (3)	—
v12j13	1783.02454	1.93 (5)·10⁻²	1.07·10⁻²	—	—	1.2 (1)·10⁻²	5.3 (3)	5.5 (9)·10⁻²
v12j12	1786.85767	9.5 (3)·10⁻³	8.6·10⁻³	—	—	1.51 (4)·10⁻²	5.2 (3)	6 (1)·10⁻²

TABLE I. Continued

Laser line	Frequency (cm^{-1})	H_2O (atm^{-1} cm^{-1})	H_2O Hitran	CO_2 (atm^{-1} cm^{-1})	CO_2 Hitran	Ethylene (atm^{-1} cm^{-1})	Acetaldehyde (atm^{-1} cm^{-1})	Ethanol (atm^{-1} cm^{-1})
v12j11	1790.65759	4.0 (1)·10⁻¹	1.86·10⁻¹	—	—	6.3 (3)·10⁻³	4.9 (3)	—
v12j10	1794.42432	3.23 (8)·10⁻²	2.92·10⁻²	—	—	4.31 (2)·10⁻³	4.0 (3)	5 (2)·10⁻²
v12j9	1798.15747	2.33 (6)·10⁻²	2.41·10⁻²	—	—	2.92 (1)·10⁻³	2.9 (2)	5 (3)·10⁻²
v12j8	1801.85693	3.94 (9)·10⁻²	4.28·10⁻²	—	—	3.891 (5)·10⁻³	2.1 (1)	4 (4)·10⁻²
v11j14	1804.3335	8.5 (4)·10⁻³	6.45·10⁻³	—	—	2.82 (3)·10⁻³	2.1 (2)	4 (2)·10⁻²
v12j7	1805.52271	1.09 (3)·10⁻²	9.51·10⁻³	—	—	2.68 (3)·10⁻³	1.6 (1)	3.7 (8)·10⁻²
v11j13	1808.23474	1.3 (4)·10⁻²	1.38·10⁻²	—	—	3.87 (8)·10⁻³	1.63 (10)	4 (2)·10⁻²
v11j12	1812.10291	6.4 (1)·10⁻²	8.27·10⁻²	—	—	3.8 (4)·10⁻³	1.37 (8)	—
v11j11	1815.93799	5.2 (2)·10⁻³	4.91·10⁻³	—	—	1.023 (4)·10⁻²	1.34 (8)	3.2 (6)·10⁻²
v11j10	1819.73962	3.2 (2)·10⁻³	2.73·10⁻³	—	—	1.11 (2)·10⁻²	1.10 (7)	2.9 (3)·10⁻²
v11j9	1823.50781	1.33 (4)·10⁻²	1.33·10⁻²	—	—	2.39 (3)·10⁻²	1.01 (6)	3 (2)·10⁻²
v11j8	1827.24231	1.6 (4)·10⁻²	1.58·10⁻²	—	—	3.09 (5)·10⁻²	1.00 (6)	3 (2)·10⁻²
v11j7	1830.94299	6.6 (2)·10⁻²	6.09·10⁻²	—	—	5.7 (2)·10⁻²	9.6 (5)·10⁻¹	4 (2)·10⁻²
v10j13	1833.52637	1.19 (3)·10⁻²	9.44·10⁻³	—	—	7.41 (9)·10⁻²	1.06 (2)	3 (2)·10⁻²
v11j6	1834.60986	1.61 (8)·10⁻²	1.21·10⁻²	—	—	9.4 (1)·10⁻²	1.04 (6)	3.0 (7)·10⁻²
v10j12	1837.42969	6.9 (2)·10⁻²	8.86·10⁻²	—	—	1.77 (4)·10⁻¹	1.03 (6)	—
v10j11	1841.29968	1.49 (4)·10⁻²	9.95·10⁻³	—	—	2.37 (9)·10⁻¹	7.5 (5)·10⁻¹	2.6 (4)·10⁻²
v10j10	1845.13635	9.9 (2)·10⁻²	9.11·10⁻²	6.5 (6)·10⁻⁵	5.98·10⁻⁵	9.38 (7)·10⁻²	6.7 (4)·10⁻¹	—
v10j9	1848.93958	1.33 (4)·10⁻²	1.27·10⁻²	3 (2)·10⁻⁶	2.8·10⁻⁶	4.57 (6)·10⁻¹	5.7 (3)·10⁻¹	2.7 (6)·10⁻²
v10j8	1852.70911	5.3 (2)·10⁻³	3.69·10⁻³	9.11 (1)·10⁻⁵	9.18·10⁻⁵	3.6 (3)·10⁻¹	4.7 (3)·10⁻¹	4 (1)·10⁻²
v10j7	1856.44482	5.9 (2)·10⁻³	3.48·10⁻³	1.3 (1)·10⁻⁵	1.06·10⁻⁵	8.06 (5)·10⁻¹	4.6 (3)·10⁻¹	4 (2)·10⁻²
v9j13	1858.89831	1.02 (3)·10⁻²	9.87·10⁻³	2.7 (1)·10⁻⁵	2.59·10⁻⁵	3.3 (5)·10⁻¹	4.7 (3)·10⁻¹	5 (3)·10⁻²
v10j6	1860.14673	5.6 (2)·10⁻³	3.39·10⁻³	4.9 (1)·10⁻⁵	1.17·10⁻⁴	6.21 (2)·10⁻¹	4.1 (3)·10⁻¹	4.5 (6)·10⁻²
v9j12	1862.83667	4.6 (2)·10⁻³	3.15·10⁻³	3.73 (7)·10⁻⁵	1.5·10⁻⁵	2.45 (2)·10⁻¹	3.3 (2)·10⁻¹	4 (3)·10⁻²
v9j11	1866.7417	5.7 (2)·10⁻²	5.22·10⁻²	1.7 (2)·10⁻⁵	1.19·10⁻⁵	5.21 (3)·10⁻¹	2.6 (1)·10⁻¹	—
v9j10	1870.6134	5.1 (2)·10⁻²	5.2·10⁻²	2.8 (3)·10⁻⁵	2.22·10⁻⁵	3.53 (3)·10⁻¹	1.8 (1)·10⁻¹	5 (4)·10⁻²
v9j9	1874.45166	2.9 (2)·10⁻³	1.93·10⁻³	5.04 (3)·10⁻⁵	3.6·10⁻⁵	4.43 (4)·10⁻¹	1.6 (1)·10⁻¹	6 (3)·10⁻²
v9j8	1878.25623	2.1 (2)·10⁻³	1.12·10⁻³	5.45 (2)·10⁻⁵	5.55·10⁻⁵	2.68 (2)·10⁻¹	1.4 (1)·10⁻¹	7 (2)·10⁻²
v9j7	1882.02698	2.3 (2)·10⁻³	1.21·10⁻³	3.93 (3)·10⁻⁵	3.64·10⁻⁵	2.22 (4)·10⁻¹	1.39 (9)·10⁻¹	8 (3)·10⁻²
v9j6	1885.76379	8.9 (3)·10⁻³	5.14·10⁻³	7.22 (4)·10⁻⁵	1.07·10⁻⁴	1.38 (1)·10⁻¹	1.2 (1)·10⁻¹	9 (3)·10⁻²
v8j12	1888.32251	4.5 (1)·10⁻²	1.13·10⁻²	4.7 (4)·10⁻⁵	3.69·10⁻⁵	1.508 (8)	1.12 (5)·10⁻¹	7 (4)·10⁻²
v8j11	1892.26257	4.0 (2)·10⁻³	3.59·10⁻³	9.6 (2)·10⁻⁵	6.44·10⁻⁵	2.21 (2)·10⁻¹	9.4 (5)·10⁻²	1.6 (4)·10⁻¹
v8j10	1896.16943	6.9 (2)·10⁻³	6.11·10⁻³	2.71 (2)·10⁻³	2.34·10⁻³	4.51 (2)·10⁻¹	7.5 (5)·10⁻²	1.5 (4)·10⁻¹
v8j9	1900.0426	1.4 (2)·10⁻³	8.52·10⁻⁴	1.91 (1)·10⁻⁴	1.83·10⁻⁴	5.68 (3)·10⁻¹	6.5 (5)·10⁻²	2.0 (6)·10⁻¹
v8j8	1903.8822	5.1 (2)·10⁻³	3.77·10⁻³	4.45 (1)·10⁻⁴	4.04·10⁻⁴	2.17 (3)·10⁻¹	8.0 (6)·10⁻²	2.2 (7)·10⁻¹
v8j7	1907.68799	5.4 (1)·10⁻²	4.59·10⁻²	6.87 (2)·10⁻⁴	5.95·10⁻⁴	2.9 (1)·10⁻¹	6.8 (1)·10⁻²	2.4 (8)·10⁻¹
v8j6	1911.45984	4.1 (2)·10⁻³	3.48·10⁻³	4.19 (6)·10⁻⁴	3.94·10⁻⁴	4.35 (7)·10⁻¹	9 (1)·10⁻²	3.1 (8)·10⁻¹
v7j12	1913.88586	4.2 (2)·10⁻³	3.56·10⁻³	1.81 (2)·10⁻³	2.09·10⁻³	9.27 (2)·10⁻¹	7.6 (7)·10⁻²	3 (1)·10⁻¹
v8j5	1915.19763	1.89 (5)·10⁻²	1.76·10⁻²	1.191 (4)·10⁻³	5.08·10⁻⁴	7.31 (7)·10⁻¹	7.1 (4)·10⁻²	4 (1)·10⁻¹
v7j11	1917.86096	7.6 (2)·10⁻¹	5.37·10⁻¹	1.261 (5)·10⁻³	1.04·10⁻³	3.69 (2)·10⁻¹	2.1 (5)·10⁻¹	3.2 (8)·10⁻¹
v7j10	1921.80286	2.15 (5)·10⁻²	1.74·10⁻²	1.33 (9)·10⁻³	1.28·10⁻³	7.0 (1)·10⁻¹	7.6 (3)·10⁻²	3 (1)·10⁻¹
v7j9	1925.71106	2.5 (2)·10⁻³	1.93·10⁻³	1.37 (1)·10⁻⁴	1.38·10⁻⁴	1.571 (4)·10⁻¹	7.6 (8)·10⁻²	3.8 (2)·10⁻¹
v7j8	1929.58569	1.1 (2)·10⁻³	6.72·10⁻⁴	1.291 (3)·10⁻⁴	1.52·10⁻⁴	2.45 (6)·10⁻¹	7.8 (5)·10⁻²	3 (1)·10⁻¹
v7j7	1933.42651	7.9 (2)·10⁻³	7.98·10⁻³	4.42 (9)·10⁻³	5·10⁻³	3.033 (9)·10⁻¹	8.2 (7)·10⁻²	4 (1)·10⁻¹
v7j6	1937.2334	2.3 (2)·10⁻³	2.27·10⁻³	1.2 (3)·10⁻⁴	1.25·10⁻⁴	9.9 (1)·10⁻²	9.5 (8)·10⁻²	2.5 (7)·10⁻¹
v6j12	1939.52515	2 (2)·10⁻³	1.6·10⁻³	3.15 (4)·10⁻⁴	3.43·10⁻⁴	8.78 (5)·10⁻²	9.5 (9)·10⁻²	3 (1)·10⁻¹
v6j11	1943.5354	1.34 (3)·10⁻²	1.21·10⁻²	—	—	6.1 (6)·10⁻²	1.05 (7)·10⁻¹	3.0 (9)·10⁻¹
v6j10	1947.51221	2.2 (2)·10⁻³	1.89·10⁻³	1.35 (1)·10⁻⁴	1.13·10⁻⁴	3.93 (9)·10⁻²	1.3 (1)·10⁻¹	3 (1)·10⁻¹
v6j9	1951.45544	8 (2)·10⁻⁴	6.26·10⁻⁴	5.27 (2)·10⁻⁵	4.1·10⁻⁵	2.46 (2)·10⁻²	1.3 (1)·10⁻¹	2.3 (8)·10⁻¹
v6j8	1955.36511	7.9 (2)·10⁻³	6.8·10⁻³	1.23 (1)·10⁻⁴	1.27·10⁻⁴	1.134 (5)·10⁻²	1.3 (1)·10⁻¹	1.9 (6)·10⁻¹
v6j7	1959.24097	9 (2)·10⁻⁴	5.08·10⁻⁴	4.05 (9)·10⁻⁵	4.16·10⁻⁵	7.52 (2)·10⁻³	1.5 (2)·10⁻¹	1.4 (5)·10⁻¹
v6j6	1963.08276	1.5 (2)·10⁻³	6.48·10⁻⁴	3.3 (4)·10⁻⁵	3.36·10⁻⁵	1.601 (7)·10⁻²	1.9 (2)·10⁻¹	1.3 (5)·10⁻¹
v5j12	1965.23877	2.8 (2)·10⁻³	2.19·10⁻³	6 (3)·10⁻⁴	6.15·10⁻⁴	1.27 (3)·10⁻²	2.0 (2)·10⁻¹	1.3 (8)·10⁻¹
v6j5	1966.89063	1.7 (6)·10⁻²	1.52·10⁻²	—	—	1.19 (2)·10⁻²	2.3 (4)·10⁻¹	1.2 (4)·10⁻¹
v5j11	1969.28394	2.0 (2)·10⁻³	1.68·10⁻³	—	—	1.444 (9)·10⁻²	2.1 (2)·10⁻¹	1.4 (5)·10⁻¹
v5j10	1973.29578	4 (2)·10⁻⁴	2.88·10⁻⁴	7.59 (2)·10⁻⁵	6.39·10⁻⁵	1.904 (7)·10⁻²	2.0 (2)·10⁻¹	1.1 (3)·10⁻¹
v5j9	1977.27417	3 (2)·10⁻⁴	2.95·10⁻⁴	9.53 (6)·10⁻⁶	1.04·10⁻⁵	1.39 (8)·10⁻²	1.8 (2)·10⁻¹	9 (4)·10⁻²
v5j8	1981.21887	1.2 (2)·10⁻³	4.7·10⁻⁴	—	—	1.511 (6)·10⁻²	1.8 (2)·10⁻¹	7 (3)·10⁻²
v5j7	1985.12964	7.1 (9)·10⁻³	4.11·10⁻⁴	—	—	1.78 (2)·10⁻²	—	—
v4j12	1991.02502	8.9 (4)·10⁻³	5.69·10⁻³	—	—	2.64 (3)·10⁻²	2.3 (3)·10⁻¹	1.0 (4)·10⁻¹
v4j11	1995.10523	4 (1)·10⁻³	8.16·10⁻⁴	—	—	4.28 (7)·10⁻²	2.3 (3)·10⁻¹	8.9 (7)·10⁻²

of the trap is being operated. This condition is partly due to a slow release of the highly polar water molecules that have formed molecular layers on the resonator walls and tubing. The relative H_2O absorption coefficients were determined by flowing the carrier gas through the cold trap set at a relatively high temperature, providing a water concentration of about 1000 ppm. However, this approach resulted in reduced intracavity laser power levels at frequencies corresponding to strong water absorption. Therefore, measurements at a lower water concentration of about 10 ppm were used for those laser lines. A constant background signal of 50 μV/W was consistently subtracted from the measured data. Absolute values for the absorption coefficients were obtained by scaling the

data to the values obtained from the Hitran 1996 database[20] with the use of a least-squares fit on 160 data points ($R = 0.995$).

CO_2 possesses a medium absorption (3 ν_2 band) at 1932 cm^{-1} and a weaker absorption band around 1400 cm^{-1}. The highest CO_2 absorption coefficient is approximately 1000 times smaller than that of the other gases, and therefore a much higher concentration was used. A mixture of 1.56% CO_2 in the carrier was produced online by using electronic mass flow controllers (Brooks 5850, Veenendaal, the Netherlands). Scaling our values to the absorption coefficients from the Hitran 1996 database (where available) with the use of a least-squares fit on 36 data points ($R = 0.992$) yielded absolute values.

Ethanol shows a strongly absorbing in-plane OH bending mode around 1400 cm^{-1} and a much weaker absorption around 1900 cm^{-1}. Acetaldehyde possesses a very strong absorption band due to the ν_4 C=O stretching mode centered at 1774 cm^{-1} and exhibits in addition a few weaker absorptions between 1400 and 1500 cm^{-1}.[21] The strong ν_4 band with a maximum absorption coefficient of 23 atm^{-1} cm^{-1} yields a detection limit of around 100 ppt for acetaldehyde in N_2. Relative absorption coefficients for ethanol and acetaldehyde were determined by applying a constant flow of carrier gas (air or nitrogen) through a small glass container containing a smaller bottle with the liquid sample. A number of small needles in the cap of the inner bottle act as diffusion channels to control the concentration of the sample. The measurement was initiated when the concentration (typically a few hundred parts per million) in a flow was constant. Since ethanol absorbs very weakly between 1600 and 1800 cm^{-1}, a higher concentration was used in this wavelength region to obtain reliable absorption coefficients here, too.

Ethylene possesses a strong absorption band due to the ν_{12} scissoring mode centered at 1444 cm^{-1} and in addition a slightly weaker absorption near 1889 cm^{-1} due to the $\nu_7 + \nu_8$ combination band.[22] The absorption coefficients for ethylene were determined by mixing, with the use of electronic mass flow controllers, gaseous ethylene with the carrier gas to a concentration of a few hundred parts per million.

A scan over all 223 laser lines (only 202 laser lines are included in Table I) takes about one hour. During the first few hours, the water concentration decreases rapidly, which is associated with cells becoming drier owing to the cold trap. For this reason, the first two or three scans were always rejected. The relative absorption coefficients were corrected by subtracting both the background signal and the contribution of water vapor from the PA spectra.

In order to obtain absolute values for absorption coefficients of selected trace gases, the PA cell response was first calibrated by using a mixture containing a known concentration of CO_2 in nitrogen and by scaling the data to the CO_2 absorption coefficients from the Hitran 1996 database. The H_2O and CO_2 absorption coefficients were calculated from the database by taking into account homogeneous pressure broadening using a Lorentzian line shape function. Subsequently, at specific laser lines the PA signal generated by a certified gas mixture of ethanol (purchased from Scott Specialty Gases, 50.9 ± 5% ppm in nitrogen) and ethylene (purchased from Praxair, 1.04 ppm in nitrogen) was recorded. The calibrated PA cell response allows a direct determination of absolute absorption coefficients because the concentration of trace gases is known. Absolute absorption coefficients for acetaldehyde were determined in a similar manner; however, instead of a certified mixture, an injection of a known amount of vapor into a nitrogen flow was used to obtain an absolute calibration.

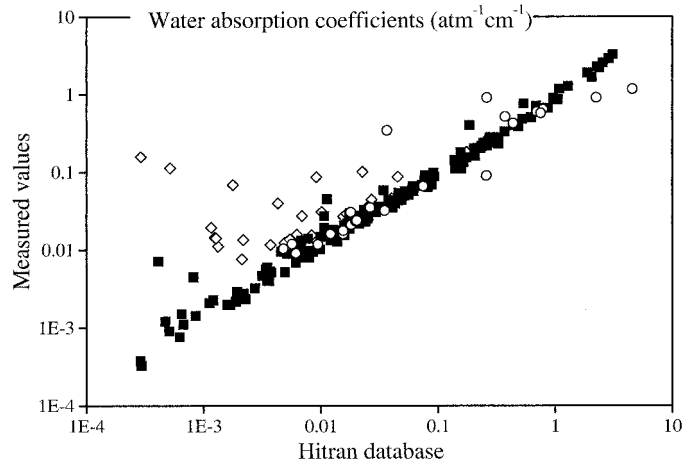

FIG. 2. Measured absorption coefficients for water vapor plotted against the values obtained from the Hitran database. (■) Laser lines between 1400 and 2000 cm^{-1}; (○) nearly coinciding laser lines between 1400 and 2000 cm^{-1} in the case of overlapping vibrational bands; and (◇) laser lines between 1300 and 1400 cm^{-1}.

The absorption coefficients for H_2O, CO_2, ethanol, acetaldehyde, and ethylene gases are tabulated in Table I (including the standard deviation). Likewise, the calculated absorption coefficients of H_2O and CO_2 from the Hitran 1996 database are also shown in Table I.

The H_2O measurements are in reasonable agreement with the Hitran data except for a region below 1400 cm^{-1} and for the case of overlapping vibrational CO bands (in Table I and Fig. 2). After rejection of low-power laser lines and those showing multiple-line emission (leaving 168 laser lines), 67% of the measured absorption coefficients are within 20% of the values as calculated from the Hitran database. Below 1400 cm^{-1}, deviations are partly due to the relatively low laser output power and a systematic error in the laser power. This error in the laser power is due to inaccuracy in the frequency-dependent ratio of the zero-order reflection of the grating and the intracavity laser power, which itself is difficult to determine precisely in the low-power region. In the case of overlapping vibrational CO bands, the CO laser may show multiple emission, and the PA signal is the sum of individual PA signals on each laser line. The ratio of these two signals depends in practice on the operating conditions of the CO laser. As an example, a discrepancy is observed when comparing measured H_2O absorption coefficients on v14j13† (1732.85254 cm^{-1}) and v15j6 (1733.28711 cm^{-1}) and the calculated values (Table I). Figure 2 shows clearly for the case of overlapping vibrational bands, that calculated and experimentally obtained values deviate substantially.

Figure 3 shows the CO_2 absorption coefficients and

† Note: v = 15 → 14; j = 12 → 13.

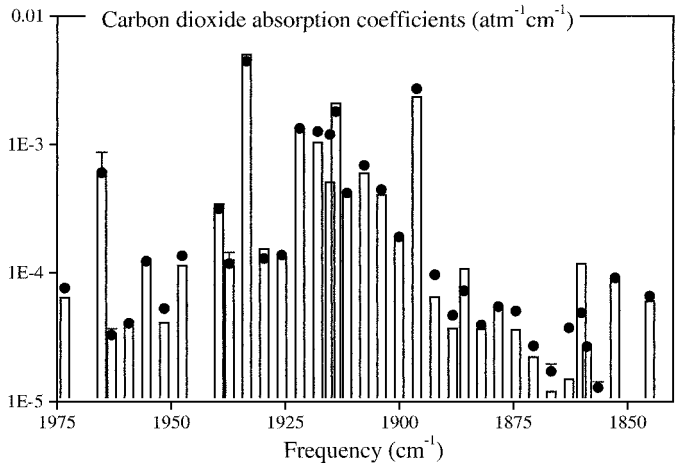

FIG. 3. Comparison between the PA spectrum (●) and the calculated Hitran infrared spectrum (□) for CO_2 gas between 1845 and 1975 cm^{-1}. Error margins refer to one standard deviation of the data. Missing error implies that the latter is smaller than the symbol size.

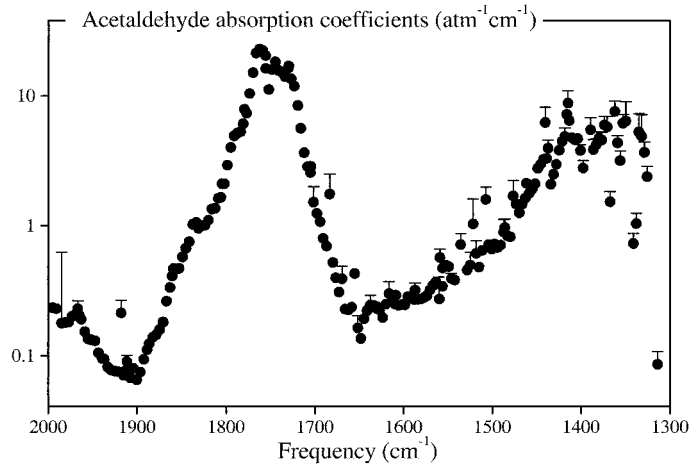

FIG. 5. The PA spectrum of acetaldehyde; error margins refer to one standard deviation of the data. Missing error implies that it is smaller than the symbol size.

data from the Hitran database between 1845 and 1975 cm^{-1}. Between 1425 and 1810 cm^{-1} no data are available in the Hitran database. The CO_2 absorption is very weak outside this wavelength region except for the small absorption around 1400 cm^{-1}. Measured CO_2 absorption coefficients in the region between 1845 and 1975 cm^{-1} are in reasonable agreement with those from the Hitran database; 68% of the 39 measured absorption coefficients are within 20% of the values calculated from the Hitran database. On many laser lines, the PA signal generated by CO_2 is even smaller than the background signal, precluding determination of the absorption coefficient at these laser lines. Due to a weak absorption of CO_2, a high concentration had to be used requiring the cold trap to be operated at a relatively high temperature. As this approach has resulted in a relatively high concentration of water in the flowing sample, no better agreement was expected. Improvement is anticipated if a chemical scrubber (such as P_2O_5) that reduces the water concentration to a few parts per million (while allowing simultaneously for high CO_2 concentration) is used.

To our knowledge, in this spectral range literature data for ethanol, acetaldehyde, and ethylene (see Figs. 4, 5, and 6) are lacking, and hence no comparison of the absorption coefficients obtained here could be made.

In the analysis of the data, three important error sources are readily recognized. First, subtraction of the PA signal generated by water vapor introduces errors, in particular for trace molecules exhibiting weak absorption on a laser line at which absorption of water vapor is high. Similarly, trace gases requiring a relatively high operation temperature of the cold trap give rise to stronger interference. Examples of the latter are ethanol and CO_2 absorption coefficients, which show larger standard deviations. Second, in the case of overlapping vibrational CO bands, the laser may show multiple line emission, with the resulting PA signal being the sum of PA signals obtained at each laser line (see Fig. 2). Finally, in the case of weak absorptions, the background signal becomes important, because the magnitude of the PA signal generated by the trace molecules becomes comparable to the background signal. In the presence of such relatively large background signals, the values of the absorption coefficients show a large uncertainty.

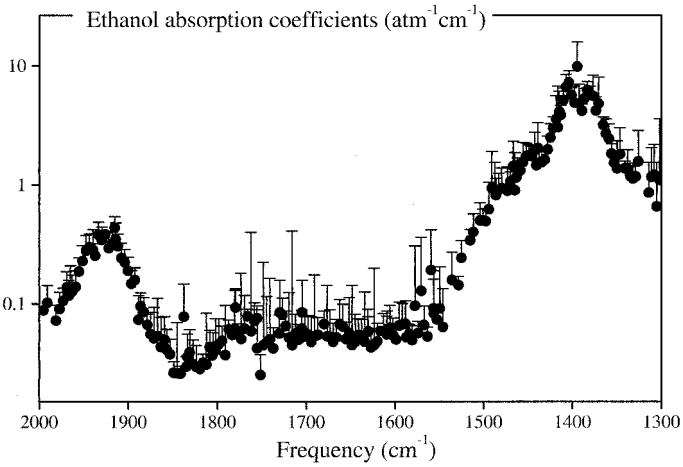

FIG. 4. The PA spectrum of ethanol; error margins refer to one standard deviation of the data. Missing error implies that the latter is smaller than the symbol size.

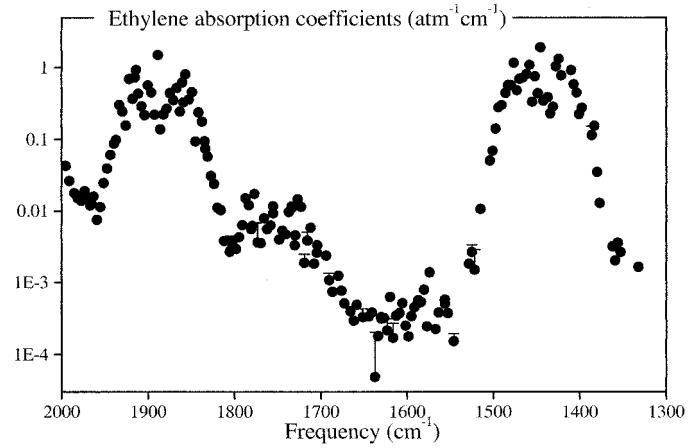

FIG. 6. The PA spectrum of ethylene; error margins refer to one standard deviation of the data. Missing error implies that the latter is smaller than the symbol size.

TABLE II. Cross sensitivities for four laser lines used in the multicomponent analysis of trace gases released by Conference pears.

Laser line	Q_{ij}				
	i↓j→	C_2H_5OH	C_2H_4	H_2O	CH_3CHO
v28j8	C_2H_5OH	**1**	0.083	0.002	0.67
v26j11	C_2H_4	0.94	**1**	0.009	1.6
v19j11	H_2O	0.13	0.0005	**1**	0.75
v13j11	CH_3CHO	0.0038	0.00038	0.0001	**1**

As compared to situations where nitrogen is used as the carrier gas, the results for trace gas mixtures in air were similar. A phase lag (up to 45°) occurred in samples with a low water content (water accelerates vibrational relaxation), indicating that relaxation properties of the gas mixture have changed. Facing a similar problem working with CO_2–N_2 gas mixtures using a CO_2 laser-based PA detector, Moeckli et al. applied a different algorithm taking into account phase information and vibrational relaxation times of the gas mixture.[23] The same algorithm can be applied here for gas mixtures containing O_2, although this approach would require accurate knowledge of the appropriate relaxation times.

MONITORING EMISSION OF TRACE GASES RELEASED BY CONFERENCE PEARS

The PA detector was used to study emission of trace gases emitted by Conference pears exposed to a flow of pure nitrogen; low emission rates of volatiles require the use of such a detection scheme. Prior to the experiment, the pears were kept in large containers under normal storage conditions (2% O_2 and 0% CO_2) for nine months.

Ethylene, H_2O, ethanol, and acetaldehyde were analyzed (interference of other gases is expected to be small) by tuning the laser to six emission lines, marked by an asterisk (*) in Table I. This selection of laser lines is based on factors such as laser power, absorption strength, and interferences. The latter can be quantitatively described in terms of mutual cross-sensitivities, as proposed by Meyer and Sigrist.[19] Cross-sensitivities Q_{ij} were computed for four laser lines at which absorptions are maximal (see Table II). Most off-diagonal elements in Table II are relatively small, indicating a low degree of mutual interference. The interference of ethylene and ethanol (Q_{12}) and that of acetaldehyde with all other trace gases (see last column) form an exception. In general, however, fruits release much less acetaldehyde than the ethanol.

A KOH scrubber was capable of removing CO_2 from the flow. In an effort to avoid early obstruction of the cold trap, sample flow was dried by means of a Nafion gas sample dryer (see Fig. 1). A fraction of the flow was led to the cold trap level kept at −70 °C (for ethanol measurements), while the remaining part was directed to the −120 °C level to detect acetaldehyde and ethylene.

A typical result obtained for a single pear (weight of 175 g) is shown in Fig. 7 (including an indication of the error). At $t = 0$ h, the pear was placed in a cuvette at 0 °C exposed to a nitrogen flow. The ethylene production rate shows a high peak at the start of the measurement; this observation is ascribed to diffusion of ethylene from the pear. Ethylene is not produced under anaerobic conditions, because O_2 is required for the ethylene biosynthesis.[14] The production rate of acetaldehyde shows a 2 h delay; after that it increases during the next 8 h. Such a pattern of acetaldehyde production during the onset of fermentation is typical and has been previously observed for tomato[16] and bell pepper.[24] After reaching a maximum, the production rate declines slightly for almost 12 h at a rate of 0.80 ± 0.02 nL/h².

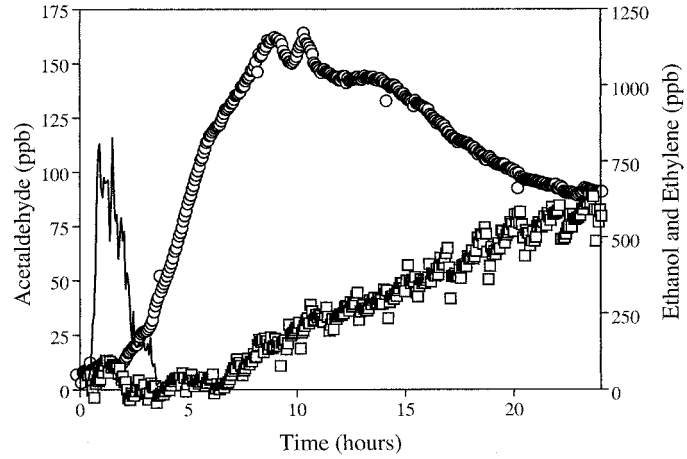

FIG. 7. Emission of acetaldehyde (○), ethanol (□), and ethylene (-) from a single pear (weight 175 g) under conditions of anoxia. The emission of ethylene is shown only for the first three hours.

Initially an artificial peak is observed in the ethanol production rate. This observation is due to ethylene interference as both ethanol and ethylene exhibit strongest absorption in the very same wavelength regions (see Table II and Figs. 4 and 6). The ethanol production rate shows a delay of approximately 7 h with respect to the onset of anoxia, after which it increases linearly (at a rate of 8.5 ± 0.2 nL/h²) during the entire experiment.

One reason for the observed delay in the onset of fermentation is a depletion of internal O_2.[24] At a flow rate of 4 L/h it takes more than 1 h for the O_2 concentration within the cuvette to drop below 0.5%. It is known that, at this O_2 level, the ratio of CO_2 release to O_2 uptake is around 2, indicating that respiration and fermentation rates are comparable.[25] The acetaldehyde and ethanol production rates are extremely low above this O_2 concentration, whereas they increase steeply below this concentration.[13] In similar experiments, a cuvette was flushed (nitrogen flow of 5 L/m) for 1 min, reducing the onset of fermentation from 2 to 1 h. Measurements of internal O_2 are planned to determine time period needed to establish anoxia within the pear after switching to anaerobic conditions.[24]

CONCLUSION

The absorption coefficients of water vapor, carbon dioxide, ethylene, ethanol, and acetaldehyde at CO laser frequencies have been determined with the use of a CO laser-based PA spectrometer. Measured absorption coefficients for CO_2 and H_2O agree reasonably well with data in the Hitran database. For laser lines showing multiple emission or having an intracavity power below about 0.3 W, agreement is less favorable. Comparison of calculated and measured H_2O absorption coefficients shows the presence of a systematic error in the long wavelength

region. Most likely this result is caused by the inaccurate determination of the frequency-dependent ratio of the zero-order reflection and the intracavity laser power. However, with the present data it will be possible to correct this ratio on the basis of the observed and calculated H_2O absorption coefficients.

Measured spectra were used in a simultaneous multicomponent analysis of trace gases released by Conference pears. A three-level cold trap made it possible to detect four trace gases at parts-per-billion concentration levels (and sub-ppb acetaldehyde). PA detectors based on liquid nitrogen-cooled CO lasers are relatively large and therefore not appropriate for field measurements (e.g., a fruit storage room). Recently, small high-power solid-state light sources have been developed and applied in PA experiments; e.g., Paldus et al. used a continuous-wave (CW) quantum-cascade laser detecting ammonia and water vapor,[26] while Kühnemann et al. measured ethane, methane, and ethylene using a CW optical parametric oscillator.[27] Fehér et al. used a near-infrared laser diode attaining a sensitivity of 8 ppb for ammonia.[28] In the near future, detection limits of these systems may become comparable to those of gas laser-based PA detectors, making them perfectly suited for field measurements.

ACKNOWLEDGMENTS

We gratefully acknowledge the technical support of C. Sikkens, C. Timmer, and H. Schoutissen. We thank the Royal Dutch Academy of Sciences KNAW (Project No. 95BTM-04), the Dutch Technology Foundation STW (applied science division of NWO) and the technology program of the Ministry of Economic Affairs for financial support.

1. A. G. Bell, Am. J. Sci. **20,** 305 (1880).
2. E. L. Kerr and J. G. Atwood, Appl. Opt. **7,** 915 (1968).
3. F. Harren, J. Reuss, E. J. Woltering, and D. D. Bicanic, Appl. Spectrosc. **44,** 1360 (1990).
4. S. te Lintel Hekkert, M. J. Staal, R. H. M. Nabben, H. Zuckermann, S. Persijn, L. J. Stal, L. A. C. J. Voesenek, F. J. M. Harren, J. Reuss, and D. H. Parker, Instrumen. Sci. Technol. **26,** 157 (1998).
5. S. Bernegger and M. W. Sigrist, Infrared Phys. **30,** 375 (1990).
6. F. G. C. Bijnen, F. J. M. Harren, J. H. P. Hackstein, and J. Reuss, Appl. Opt. **35,** 5357 (1996).
7. G. D. T. Tejwani, J. Quant. Spectrosc. Radiat. Transfer **40,** 605 (1988).
8. K. M. T. Yamada, M. Harter, and T. Giesen, J. Mol. Spectrosc. **157,** 84 (1993).
9. T. Giesen, R. Schieder, G. Winnewisser, and K. M. T. Yamada, J. Mol. Spectrosc. **153,** 406 (1992).
10. A. Gerasimchuk, S. Kornilov, I. Ostrejkovskij, E. Protsenko, and S. Tymper, Appl. Phys. B **55,** 503 (1992).
11. W. Schnell and G. Fischer, Opt. Lett. **2,** 67 (1978).
12. R. T. Menzies and M. S. Shumate, Appl. Opt. **15,** 2080 (1976).
13. H. W. Peppelenbos, Ph.D. Thesis, Landbouw Universiteit, Wageningen (1996).
14. F. B. Abeles, P. W. Morgan, and M. E. Salveit, Jr., *Ethylene in Plant Biology* (Academic Press, London, 1992), 2nd ed., Chap. 3, pp. 42–43.
15. H. Zuckermann, F. J. M. Harren, J. Reuss, and D. H. Parker, Plant Physiol. **113,** 925 (1997).
16. F. G. C. Bijnen, H. Zuckermann, F. J. M. Harren, and J. Reuss, Appl. Opt. **37,** 3345 (1998).
17. F. G. C. Bijnen, J. Reuss, and F. J. M. Harren, Rev. Sci. Instrum. **67,** 2914 (1996).
18. W. Urban, in *Frontiers of Laser Spectroscopy of Gases,* NATO-ASI Series, A. C. P. Alves, J. M. Brown, and M. Hollas, Eds. (Kluwer Academic Publishers, Dordrecht, 1988), pp. 9–42.
19. P. L. Meyer and M. W. Sigrist, Rev. Sci. Instrum. **61,** 1779 (1990).
20. Hitran Atmospheric Workstation for Windows (Ontar Corporation, North Andover, Massachusetts, 1996).
21. K. B. Wiberg, Y. Thiel, L. Goodman, and J. Leszczynski, J. Phys. Chem. **99,** 13850 (1995).
22. D. van Lerberghe and A. Fayt, Mol. Phys. **31,** 1875 (1976).
23. M. A. Moeckli, C. Hilbes, and M. W. Sigrist, Appl. Phys. B **67,** 449 (1998).
24. J. Oomens, H. Zuckermann, S. Persijn, D. H. Parker, and F. J. M. Harren, Appl. Phys. B **67,** 459 (1998).
25. H. W. Peppelenbos, private communication.
26. B. A. Paldus, T. G. Spence, R. N. Zare, J. Oomens, F. J. M. Harren, D. H. Parker, C. Gmachl, F. Cappasso, D. L. Sivco, J. N. Baillargeon, A. L. Hutchinson, and A. Y. Cho, Opt. Lett. **24,** 178 (1999).
27. F. Kühnemann, K. Schneider, A. Hecker, A. A. E. Martis, W. Urban, S. Schiller, and J. Mlynek, Appl. Phys. B **66,** 741 (1998).
28. M. Fehér, Y. Jiang, J. P. Maier, and A. Miklós, Appl. Opt. **33,** 1655 (1994).